

Parametric Analysis in Power Engineering

PEBN #11 (Nov. 2008)

W.L. Soong
 School of Electrical and Electronic Engineering
 University of Adelaide, Australia
 soong@ieee.org

Abstract – a powerful approach to understanding the characteristics of engineering systems is to show their performance using graphs of carefully chosen dimensionless parameters. This technique is illustrated using two case studies : a full-wave rectifier and unbalanced magnetic pull.

I. INTRODUCTION

This brief illustrates the concept of parametric analysis using two case studies. These case studies describe the selection of the dimensionless parameters based on a physical understanding of the effect of each input variable on the output quantity being studied. These dimensionless parameters are chosen to capture as many of the system variables as possible.

It should be noted that while the use of dimensionless parameters has a certain similarity to per-unit systems, it is significantly different. A key aspect of per-unit systems is the choice of a small number of primary base values (e.g. power and voltage) which can be used to derive a mathematically consistent set of secondary base values. For the dimensionless parameters described, the emphasis is more using these parameters for physical understanding of the problem rather than mathematical calculations.

II. FULL-WAVE RECTIFIER CASE STUDY

Consider a full-wave rectifier circuit with an AC sinusoidal input voltage v_s of amplitude V_{pk} and period T . It is connected through a diode to a parallel combination of a filter capacitor C and resistive load R . The diodes can be modelled as a constant voltage drop V_d when conducting.

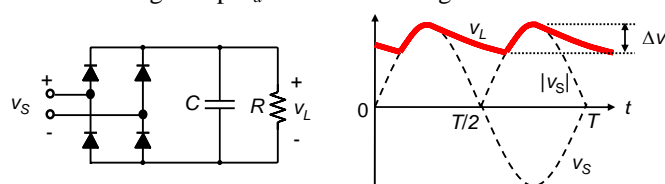


Fig. 1. Full-wave rectifier circuit diagram (left) and idealised output voltage waveform (right).

Ignoring the diode voltage drop, the circuit operates as follows : when the input voltage magnitude is greater than the output voltage then the diodes turn on and the AC voltage source charges the capacitor and supplies the load current. When the input voltage magnitude is less than the output voltage, the diodes turn off and the capacitor discharges through the load resistance producing an output voltage which decays exponentially with time constant $\tau = RC$. The circuit has a peak-to-peak output voltage ripple Δv .

It is desired to investigate how the output voltage ripple Δv varies as a function of the five circuit parameters V_{pk} , T , R , C and V_d . The first step is to recognize that all the parameters have a first-order effect on the output ripple voltage apart from

V_d which has a second-order effect. We will thus neglect V_d initially.

Next, let us pick arbitrary values for the first-order parameters V_{pk} , T and R , for instance 10 V, 20 ms and 10 ohms, respectively. It is now possible to produce a plot of the output ripple voltage Δv versus C using analytical or numerical circuit analysis methods for a range of values of C . The resulting curve is shown in Fig. 2. Clearly this plot is only accurate for the chosen values of V_{pk} , T and R .

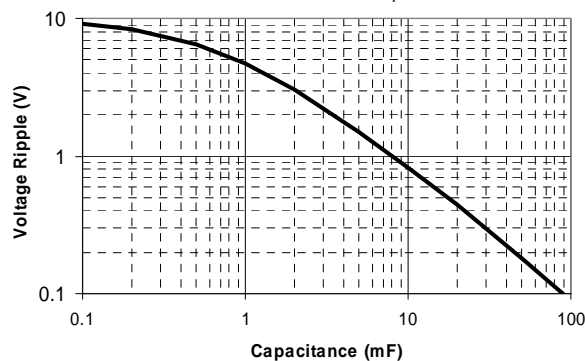


Fig. 2. Ripple voltage (Δv) versus capacitance (C), for $V_{pk} = 10V$, $T = 20ms$ and $R = 10\Omega$.

Given the output voltage of the system scales linearly with input voltage V_{pk} , instead of plotting Δv we can use the dimensionless parameter $\Delta v/V_{pk}$ which makes the curve valid for any value of V_{pk} . In addition, instead of plotting the graph using capacitance C , we use the fact that the ripple voltage is really a function of the decay time-constant RC rather than R or C . Finally by scaling the time axis of the simulations, we can show that the ripple voltage is a function of the time-constant RC with respect to the supply period T . Thus we obtain the fully parametric solution by plotting $\Delta v/V_{pk}$ versus RC/T or T/RC .

The full parametric graph of $\Delta v/V_{pk}$ versus RC/T can be obtained by choosing arbitrary values of V_{pk} , T and R , and solving for Δv versus C (such as shown in Fig. 2), and then scaling the resultant graph in terms of the desired dimensionless quantities (see Fig. 3). This is logical because if the results are really applicable to any component values, then the general relationship can be obtained using any choice of parameters for the simulation.

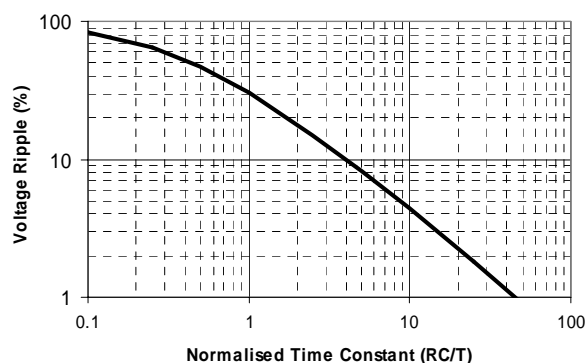


Fig. 3. Ripple voltage ($\Delta v/V_{pk}$) versus normalised filter time-constant (RC/T).

To take into account the second-order effect of the diode voltage drop we can plot curves for the above graph for different values of the dimensionless parameter V_d/V_{pk} .

III. UNBALANCED MAGNETIC PULL

Another example of the use of dimensionless parameters is in the analysis of unbalanced radial magnetic forces in electrical machines produced by eccentricity.

Consider the idealised case of an electrical machine with a smooth (non-slotted) cylindrical stator and rotor, and a sinusoidally distributed airgap winding. The machine has an airgap radius r , stack length l and a small airgap of length g . The three-phase airgap winding has N_s turns per phase, has p pole-pairs, and is carrying a peak current of I_{pk} .

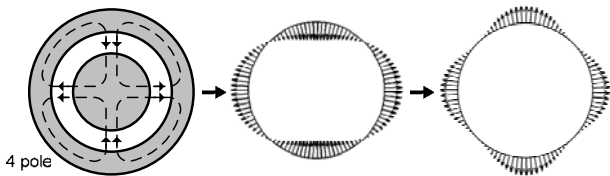


Fig. 4. Four-pole flux pattern (left), radial airgap flux density waveform (middle), and radial force distribution (right) with the rotor centred.

The airgap winding generates a sinusoidally-varying flux density waveform around the airgap with a peak value of B_{pk} . When the rotor is centred this flux density distribution is balanced, that is, the magnitudes of the flux density on opposite sides of the rotor are equal.

The airgap flux density produces a force of attraction between the rotor and stator. With a balanced flux density distribution, the magnitudes of the force on opposite sides of the rotor are equal and hence the net force on the rotor is zero.

If the rotor is shifted from its centred position by Δg , then the airgap around the rotor becomes non-uniform (eccentric). This increases the flux density in the region where the airgap is smaller and decreases it where the airgap is large. The result is an unbalanced flux density distribution and hence a net force on the rotor F . This force is termed unbalanced magnetic pull (UMP) and is shown in Fig. 5 as a function of the rotor eccentricity Δg .

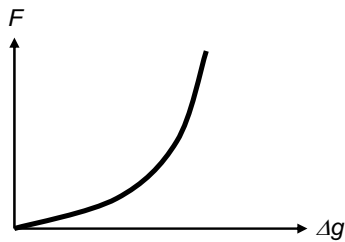


Fig. 5. Graph of UMP force versus eccentricity Δg .

The net force on the rotor F is a function of r , l , g , B_{pk} , p and Δg . Note the use of the peak airgap flux density under centred rotor conditions B_{pk} , which is more physically meaningful than the parameters N_s and I_{pk} .

The first step is to normalise the rotor eccentricity Δg . This could be normalised against the rotor radius, for instance $\Delta g/r$, but a better choice would be $\Delta g/g$ as it is this change in airgap length relative to the nominal airgap length which affects the unbalanced magnetic field distribution.

The second step is to normalise the net force on the rotor. This can capture the effects of varying the parameters r , l and B_{pk} . One approach is to assume the rotor really consists of two halves joined together and to calculate the force F_0 pulling the two halves apart when the rotor is in its centred position using analytical or numerical methods. This can be calculated for a

particular number of poles, or it can be done assuming the flux density magnitude is constant around the rotor surface.

Using these results we can now produce a parametric curve showing the variation of F/F_0 versus $\Delta g/g$. Curves can be produced for different number of poles $2p$. Saturation can also be included by consider a saturation flux density B_{sat} . We can thus plot F/F_0 versus $\Delta g/g$ for different values of the normalised saturation factor B_{sat}/B_{pk} or B_{pk}/B_{sat} as shown in Fig. 6.

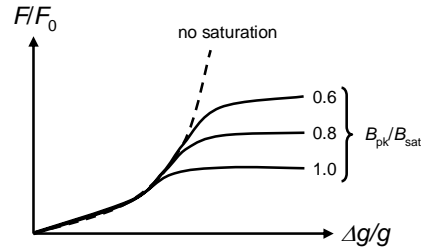


Fig. 6. Parametric graph of normalised UMP force versus normalised eccentricity as a function of the normalised saturation factor B_{pk}/B_{sat} .

IV. SUMMARY OF APPROACH

The first step in the process is to identify what is the output parameter being examined. This was output ripple for the rectifier case and radial force for the UMP case. Separate parametric graphs can be produced for other output parameters, e.g. average output voltage for the rectifier case.

Next the key input parameters which have the strongest influence on the output parameter should be identified. One of these is chosen and a plot of the output parameter (y-axis) versus this input parameter (x-axis) is produced using arbitrary values for the remaining key input parameters.

The remaining key input parameters need to be “normalised out” by combining them with either the output parameter or the parameter chosen as the x-axis of the plot. This is based on what makes the most sense physically. It may be helpful to think about whether the input parameters scale the y-axis or the x-axis and then combine them with the appropriate one.

Input parameters which cannot be normalised out, or second-order parameters, can be taken into account by plotting additional curves on the plot using further dimensionless parameters as shown in Fig. 6.

Finally it may be helpful to “modify” the x- or y-axis parameters to “linearise” the plots. For instance by plotting the square, logarithm etc of the dimensionless parameter.

REFERENCES

- [1] A. Morales-Castorena, W.L. Soong and N. Ertugrul, “Radial Force in Ideal Maxwell-Force Bearingless Motors Principle of Operation and Modelling,” IEEE RVPAI conference, 2007.

A WORD FOR TODAY

These are the wise sayings of Solomon, David's son, Israel's king— written down so we'll know how to live well and right, to understand what life means and where it's going; A manual for living, for learning what's right and just and fair; To teach the inexperienced the ropes and give our young people a grasp on reality. There's something here also for seasoned men and women, still a thing or two for the experienced to learn—fresh wisdom to probe and penetrate, the rhymes and reasons of wise men and women.
 Proverbs 1:1-6 (The Message)